DOI: 10.36108/ujees/2202.40.0172

UNIOSUN Journal of Engineering and Environmental Sciences. Vol. 4 No. 1. March. 2022

Development of Titanium Dioxide Pillared Clay Adsorbent for Removal of Lead (II), Zinc (II), and Copper (II) ions from Aqueous Solution

Ajala, M.A., Ajala, E.O., Tayo-Alabi, A., Sodiq, H.K., Abdulkareem, A.S., Kovo, A.S. and Tijani, J.O.

Abstract: The removal of heavy metals from an aqueous solution using titanium dioxide pillared clay was investigated in this study. The clay was beneficiated and Fourier Transform Infrared spectroscopy (FTIR), X-ray diffraction (XRD), resolution scanning electron microscope (HRSEM) were used to describe its characteristics, among others. The synthesis of titanium dioxide was carried out with *Parkia biglobossa* plant extract. The functionality of the titanium dioxide-beneficiated clay (TiO_2-Bclay) was studied for metal ions adsorption from the aqueous solution. The effects of adsorbent dosage, temperature, contact time, and pH on Zn(II), Cu(II), and Pb(II) ion removal percentages from the aqueous solution were investigated. Equilibrium adsorption data were fitted into isotherms and kinetic models to test their consistency. Characterization results showed that the clay contains functional groups that can bind heavy metals and absorb other hazardous substances. The pillared TiO_2 was rutile phase, porous; it was also quite high in alumina and silica. Up to 99.00% Zn(II), 92.51% Pb(II), and 88.27% Cu(II) ions were extracted at 30°C using 20 g/L adsorbent. The adsorption kinetics was best described by the pseudo-second-order model. The titanium dioxide pillared clay was found to be effective in these experiments and adjudged effective adsorbents, for heavy metals confiscation from industrial wastewater.

Keywords: Adsorption, Characterization, Heavy metals, Isotherms, Kinetics, Nano-adsorbent Thermodynamics

I. Introduction

Water pollution due to anthropogenic activities is a global apprehension, which has caused unpleasant consequences on the survival of all living organisms. Effects of pollution include; food poisoning, ecosystem disruption, diseases, and death of organisms. As a result of toxic pollutants which include dyes, organic materials and heavy metals, released into the water bodies [1]. Heavy metals contained in industrial waste accumulate in lakes and rivers, where they are usually dumped. They have been found harmful to humans and animals by causing severe health risks and problems such as acute poisoning, cancer, acute renal and respiratory problems [2, 3]. Arsenic, cadmium, mercury, chromium, copper, lead, nickel, and zinc are the most typically discovered heavy metals in wastewater [4]. Since industrial activities cannot be terminated to reduce or eliminate heavy metals in wastewater, it is crucial to implement water treatment and purification methods to take away heavyweight metals from the generated wastewater [5].

The removal methods of heavy metals include evaporation, ion exchange, chemical precipitation, membrane filtration [6]. These methods necessitate the replacement of parts regularly, depending on the volume of water and the concentration of heavy metals, making them uneconomical. They also require a lot of energy or chemicals, especially when

Ajala, M.A., Ajala, O.E., Tayo-Alabi, A. and Sodiq, H.K. (Department of Chemical Engineering, University of Ilorin, Ilorin, Kwara State, Nigeria)
Abdulkareem, A.S. and Kovo, A.S. (Department of Chemical Engineering, Federal University of Technology, Minna, Niger State, Nigeria)
Tijani, J.O. (Department of Pure and Applied Chemistry, Federal University of Technology, Minna, Niger State, Nigeria)
Corresponding author: ajala.ma@unilorin.edu.ng
Phone Number: **+2348032429560**
Submitted: 29-01-2022
Accepted: 08-03-2022

the concentration of heavy metals is low [7, 8]. The shortcomings of these conventional wastewater treatment processes have directed attention to the need for an effective and versatile method of treatment, which is achievable in the adsorption process. Adsorption is an effective treatment process at high and low contaminant concentrations [9, 10]. It allows the use of several materials as adsorbents, ranging from plant wastes such as plantain stalks, rice husks, clay materials [11-13], and engineered materials such as nanoparticles [2, 14, 15].

The use of nanoparticles and engineered nanomaterial for heavy metals removal has gained wide acceptance because they are non-toxic, have excellent sorption capabilities, selectivity for low pollutant concentrations. They also have a relatively high contact area, efficient regeneration capabilities of the adsorbed pollutant, and recycling possibilities. Such nanomaterials are; nanotubes made from carbon, graphene and its composite, carbon material composites, polymeric sorbents, nano metallic oxides [16]. In recent years, titanium dioxide (TiO_2) has been extensively used as a water remediation adsorbent and biodiesel catalyst [17]. This is due to its optical properties, high chemical stability, nontoxicity high thermal stability, specific surface area and reactivity [18-20]. The biological synthesis of nanoparticles using green plants parts is considered the best because the process is environmentally benign, easy to use, quick to complete and cost-effective. Other advantages of the green synthesis method are the ability of the nanoparticles formed to agree with biological life and can easily be produced on a large scale due to the abundance of plants parts [21, 22]. Therefore, the green synthesis of TiO_2 nanoparticles has been reported using various green plants such as; *Cassia fisula* [23], *Azadirachta indica* leaf extract [24], *Echinacea purpurea [25], Glycyrrhiza glabra* [26], *Parkia biglobossa* [27]. The green synthesised TiO_2 nanoparticles are not without drawback as it has small particle size which gives rise to post-separation challenges. Also, according to Mishra et al. [28], using TiO_2 nanoparticles as adsorbents for wastewater treatment is ineffective due to its low surface area and porosity, as well as its difficult to separate from the reaction composition, hence less reusable. To overcome these limitations, materials such as clay can provide support for TiO_2 nanoparticles.

Clays have gained immense attention due to their high availability in the earth's crust; they are cheap and retain high thermal stability as well as chemical and mechanical stability [28]. Examples of such clays are montmorillonite, bentonites and kaolinites which have been explored for the removal of heavy metals from aqueous solutions. This is due to their outstanding properties such as cation exchange capacity, negative surface charge, and high surface area [29]. However, utilising clay without modification with nanoparticles for the removal of heavy metals and other pollutants from wastewater shows low removal capacities for pollutants [30]. Hence, the pillaring of clay with TiO_2 nanoparticles would enhance the available surface area for a more efficient adsorptive removal of pollutants compared to the individual use of either clay or TiO_2. This is because clays provide TiO_2 with high surface area, porosity, a high number of surface active sites which makes TiO_2/clay nanocomposites highly active in wastewater treatment compared with pure TiO_2 [28].

Several researchers have reported the use of TiO_2/clay nanocomposites for wastewater treatment with commensurate excellent performance. Sharififard *et al.* [20] utilised commercially available nanoclay modified with TiO_2 for the removal of cadmium from wastewater solutions. A good adsorption

capacity of 16.20 mg/g was obtained for cadmium when a nanoclay/TiO_2 adsorbent was employed, although a commercially purchased clay was used for their adsorbent development. The efficiency of TiO_2-smectite clay was also tested successfully for the removal of fluorescein (dye) and p-nitrophenol (pesticide) pollutants from wastewater [30]. Though raw clay was used to develop their adsorbent, titanium (IV) tetraisopropoxide was the precursor to develop TiO_2 nanoparticles by the sol-gel method. Also, the TiO_2/kaolinite nanocomposites reported by Awwad et al. [31] showed good promise for its use in wastewater treatments, however, their study was limited to only Pb (II) and Cd (II) ions removal. Hajjaji et al. [32] utilised TiO_2/kaolinite composites to successfully remove methylene blue and orange II dyes from simulated wastewater. Their study revealed that the TiO_2 precursor used was Degussa TiO_2, which is a commercially available anatase phase TiO_2 as well as a commercial clay source. From the aforementioned literature, none of the authors reported the use of *Parkia biglobossa* leaves extract for the green synthesis of TiO_2 nanoparticles. The use of local natural clay from *Akerebiata*, Ilorin has also not been reported in the literature for the adsorption of Zn (II), Pb (II) and Cu (II) ions from wastewater, hence, the novelty of this study.

Therefore, this study considers the green synthesis of titanium dioxide supported on beneficiated clay to remove selected heavyweight metals from an aqueous solution. The TiO_2/Bclay nanocomposites developed in this study as adsorbent was characterised by X-ray diffraction (XRD), Fourier transmission infrared (FTIR) and scanning electron microscope (SEM). A batch adsorption study was also carried out for the adsorption of Zn (II), Pb (II) and Cu (II) ions from pharmaceutical wastewater under variables such as pH, contact time and adsorbent dosage. The kinetics, isotherms and thermodynamic studies of the batch adsorption process were investigated.

II. Materials and Methods

A. Materials

The clay for the present work was collected from a local clay deposit at Akerebiata, Ilorin East, Nigeria (Lat/Long: 8°.34'16"N/4°.43'42"E). The location is an abundant clay deposit, where local pottery fabricators collect clay samples for their use. *Parkia biglobosa* leaves were collected from the University of Ilorin environs. Titanium Hydroxide $TiO(OH)_2$ used was manufactured by Guangzhou Jhd Chemical Reagent Co., Ltd. (JHD) China; HCl, NaOH, $ZnSO_4.7H_2O$, $Cu(NO_3)_2$, and $Pb(NO_3)_2$ salts purchased from Merck chemicals, India. These were used to prepare Zn(II), Pb(II), and Cu(II) ions in a standard solution to serve as simulated wastewater. All of the chemicals/reagents utilized were of the highest analytical quality and had a high percentage of purity.

B. Experimental

i. Clay Beneficiation

The clay was beneficiated to remove impurities and the clay solution was passed through a screen of mesh size BSS 100 to obtain fine particles. The particles were air-dried to remove moisture and dry clay was ground to a fine powder. Clay particles were characterized by physicochemical techniques such as Fourier Transform Infrared (FTIR) analysis, X-ray diffraction (XRD), and scanning electron microscopy coupled with energy dispersive spectroscopy (SEM/EDS).

ii. Preparation of Plant Extract

The plant extract was prepared to adopt the method of Ajala *et al.* [27] as follows; the *P.biglobosa* were de-stalked and the leaves were

room dried away from sunlight to prevent loss of the delicate plant phytochemicals for 14 days. After which they were ground and sieved to obtain a fine powder. The phytochemical analysis of phenol, flavonoid, and tannin of the fine powder of each plant was conducted. The plant extract was prepared by adding 10 g pulverized dried leaves of *P. biglobosa* into a conical flask containing 100 mL of water distilled water and placed on a heated magnetic stirrer at 50℃ for 10 minutes to extract the phytochemical constituents needed as reducing agent. The mixture was allowed to cool, and the leaf extract was obtained by filtering through the Whatman filter paper. The aqueous leaves extracted were directly used for the TiO_2 nanoparticles synthesis or stored in a refrigerator (4°C) for further experiments.

iii. Preparation of 0.5 M Titanium Hydroxide Solution

Titanium hydroxide ($TiO(OH)_2$) of 14.5 g was weighed and transferred into a 250 cm^3 standard flask. Deionized water was poured to half the volume of the standard flask, and a white suspension was obtained. It was vigorously shaken for 30 minutes, after which the solution was made up to the flask mark. It was directly used in synthesising TiO_2 nanoparticles or stored at room temperature for additional experiments.

iv. Green Synthesis of TiO_2 Nanoparticles

Nanoparticles of titanium dioxide were synthesized by adopting and modifying the method of Ajala *et al.* [27] and Zahir *et al.* [33] but with $TiO(OH)_2$ precursor. Titanium nanoparticles were prepared using varying concentrations of plant extract and precursor solution and stirring speed using the same precursor concentrations, temperature, time, and pH. Synthesis mixture (plant extract and precursor) was maintained with a stirring time of 2 h.

The resulting mixture containing titanium hydroxide solution and leaf extract in a beaker was stirred on a magnetic stirrer at 35 ℃ at pH 8. The light green colour was obtained by adding plant extract into the titanium hydroxide solution. After continuous stirring, the colour changed from light green to brown, which indicates the formation of titanium nanoparticles. The titanium nanoparticles were washed with deionized water during filtration using Whatman filter paper and were collected after washing. The residue was left to age overnight, dehydrated in the oven at 100 °C for 1 hour, and calcined at 550 °C in a muffle furnace for 2 hours.

v. Synthesis of TiO_2 Pillared Clay

The TiO_2- pillaredclay particles was produced by directly incorporating clay with titanium hydroxide. This was carried out by adding 100 cm^3 of plant extract and 100 cm^3 of 0.5 M titanium hydroxide into an Erlenmeyer flask. A magnetic stirrer was used to agitate the mixture for 2 h at minimum agitation (1000 rpm). Adopting and modifying the work of Laysandra *et al.* [34] 40 g of clay that had been beneficiated (Bclay) was measured and poured to the titanium hydroxide solution on the magnetic stirrer, then stirred for another 2 hours for proper loading of TiO_2 into the clay. The titanium nanoparticles pillared clay (TiO_2-Bclay) was acquired by filtering with Whatman filter paper. The residue from the filter paper was air-dried for 24 hours and then dehydrated in the oven at 100 °C for 2 hours then, calcined at 550 °C in a muffle furnace for 2 h to obtain TiO_2-Bclay. The TiO_2-Bclay was characterized using FTIR, XRD, and HRSEM/EDS.

vi. Preparation of Simulated Wastewater

Wastewater from a pharmaceutical company in Ilorin was collected and the quantities in mg/L of heavyweight ions were obtained after digestion of the samples using Atomic Absorption Spectroscopy analysis. This led to the choice of Zinc, Lead, and Copper metal ions as a focus for this study due to their higher concentrations in the wastewater. Based on the results obtained from the pharmaceutical wastewater analyzed, simulated wastewater was prepared to obtain higher concentrations of metal ions. This was done to measure the effectiveness of the adsorbent. Metal ions solutions of Zn (II), Cu (II), Pb (II) respectively, containing 1000 mg/L, were made by dissolving the required amount of metal salts in the appropriate amount of deionized water. The metal salts used were $ZnSO_4.7H_2O$, $Cu(NO_3)_2$, and $Pb(NO_3)_2$. Other concentrations were made ready by serial dilutions. The amount of Zn (II), Cu (II), Pb (II) ions in simulated wastewater were specified by Atomic Adsorption Spectroscopy.

C. Adsorption Experiment

Batch adsorption studies of Zn(II), Pb(II) and Cu(II) onto TiO_2-Bclay from diluted solution was studied varying time (30, 60, 90, 120, 180, and 240 min), concentration (100, 200, 400, 600, 800 and 1000 mg/L), adsorbent dosage (1.0 g/1 to 20 g/L), pH (2-8) and temperature (30-50 ℃). A factor was varied per time to determine each effect, keeping all other parameters constant. After adsorption, the samples were filtered to separate the solution from the adsorbent using Whatman filter paper. The amounts of Zn (II), Cu (II), Pb (II) in the filtrate were determined by Atomic Adsorption Spectroscopy (AAS). The isothermal, kinetics and thermodynamic studies of the adsorption process were determined.

The quantities of Zn (II), Cu (II), Pb (II) adsorbed by the adsorbent at equilibrium condition were determined by using Equation 1:

$$q_e = \frac{v}{m}(C_O - C_e) \quad (1)$$

$\mathbf{q_e}$ (mg/g) is the equilibrium concentration of adsorbed Zn (II), Cu (II) or Pb (II), $\mathbf{Co}$ and $\mathbf{C_e}$ (mg/L) are the initial and equilibrium concentration of adsorbed Zn (II), Cu (II), or Pb (II) respectively, v (L) is the volume of aqueous solution added to the bottle, and m being the adsorbent mass (g).

D. Adsorptive Effects

The effects of contact time, adsorbent dosage and reaction temperature were determined on the uptake of the three metal ions onto the TiO_2-Bclay. 50 cm^3 of wastewater was mixed with 0.5 g of TiO_2-Bclay in a 100 mL conical flask. The solution was stirred continuously by a thermostat shaker and samples were withdrawn at 30 min intervals until the 240th min. The experiment was carried out with other parameters at constant values; 0.5 g adsorbent dosage, pH of 7 and constant initial concentration of 1000 mg/L. The supernatants were then filtered and analyzed through the Atomic Absorption Spectrophotometer. Effect of TiO_2-Bclay adsorbent dosage was studied using adsorbent dosage between 1-20 g/L, at constant conditions of 1000 mg/L concentration, 90 min time, the temperature at 30 ℃, and pH.of 7. The Effect of pH on metal ion's adsorption was considered in the range of pH between 2.0 and 10.0, keeping other conditions constant. Effect of temperature of adsorption medium was also carried out, varying the temperatures between 30, 40, and 50 ℃ respectively.

E. Digestion of Samples

After the adsorption process was completed in the thermostatic water bath, the sample was hydrolyzed before analysis using Atomic Absorption Spectroscopy (AAS) by digestion of samples with the aqua region (HNO_3 67%: HCl 37% in 3:1). The digestion was done by adding concentrated HNO_3, concentrated HCl, and sample solution in the ratio of 3:1:1 in a beaker. The sample was heated at 100 °C for 20–30 minutes on a hot plate until a clear solution was obtained. The solution was then allowed to cool, filtered using Whatman filter paper, and transferred to a 50 mL graduated measuring cylinder. The beaker was rinsed to remove any bulk material using deionized water, and the solution was poured into a graduated measuring cylinder. The solution was made up to a mark of 50 cm^3. The solution was then transferred into sample bottles and capped before AAS analysis.

F. Isothermal Models

i. Freundlich Isotherm

The Freundlich isotherm model [35], is an experimental equation given by **Eqn. 2** as a term frequently used to describe the adsorption of ions/molecules on a heterogeneous surface and is based on sorption on solid adsorbent surfaces.

$$\mathrm{q_e} = \mathrm{K_F C_e^{\frac{1}{n}}} \quad (2)$$

Where $\mathrm{q_e}$ is the quantity of the particular ion sorbed per unit mass of adsorbent (mg/g), K_F and n are the Freundlich constants linked to adsorption capacity and adsorption intensity, while Ce is the equilibrium concentration of an unadsorbed metal ion in the filtered solution at equilibrium (mg/L).

ii. Langmuir Isotherm

Langmuir isotherm [36] given by **Eqn. 3** based on the simplest model of physical adsorption. The isotherm assumes that the molecules are adsorbed at each discrete site of the surface where only one molecule is adsorbed.

$$q_e = q_{max}\left(\frac{K_L C_e}{1+K_L C_e}\right) \quad (3)$$

Where q_{max} and K_L (two Langmuir parameters) represent the maximum adsorption capacity and a constant attributed to the sorption of the binding sites.

iii. Dubinin-Radushkevich Isotherm

Dubinin-Radushkevich isotherm model describes whether the adsorption occurred by chemical or physical processes. The model is given by **Eqn. 4**

$$\frac{\mathrm{q_e}}{\mathrm{q_{mDR}}} = e\,\mathrm{xp}(-K_{DR}\varepsilon^2) \quad (4)$$

Where $\varepsilon = \mathrm{RT\ln}\left(1+\frac{1}{C_e}\right)$ and q_{mDR} represents the maximum adsorption of the adsorbent (mg/g), R is the gas constant (8.314 J/mol.K), T is the temperature (K). K_{DR}, Dubinin–Radushkevich constant (mol^2/kJ^2), and ε represents the Polanyi potential (J/mol). The linearized form of Dubinin-Radushkevich isotherm is given by **Eqn. 5**

$$\ln \mathrm{q_e} = \ln \mathrm{q_{mDR}} - K_{DR}\varepsilon 2 \quad (5)$$

The values of K_{DR} and q_{mDR} are obtained from the linear relationship between $\ln q_e\ vs\ \varepsilon^2$ also, the mean free energy of adsorption, E (mol/kJ), is calculated from K_{DR} **Eqn. 6**

$$E = \frac{1}{\sqrt{2K_{DR}}} \quad (6)$$

iv. Temkin Isotherm

The Temkin isotherm model, which implies that the adsorption energy decreases linearly with surface coverage due to adsorbent-adsorbate interactions, was also utilized to compute the adsorption data. The linearized version is expressed by **Eqn. 7**.

$$q_e = \frac{RT}{b_T} \ln K_T + \frac{RT}{b_T} \ln C_e \quad (7)$$

The Temkin isotherm constants K_T (L/g), b_T (J/mol), and R (8.314 J/mol.K) are all constants linked to the heat of sorption.

G. Adsorption Kinetics

Several kinetic models are used to investigate the mechanisms of metal adsorption processes and the main parameters affecting sorption generally [27]. Two of these were utilized in the present study namely: Pseudo first order and Pseudo second order kinetics model.

The Pseudo first order, popularly called pseudo-first-order expression is expressed by the **Eqn. 8**

$$\log(q_e - q_t) = \log q_e - \frac{k_1}{2.303} t \quad (8)$$

Where q_e is equilibrium capacity concentration of adsorbate (mg/g), q_t is the amount adsorbed at any time and k_1 is the first-order rate constant of adsorption (g/mg·min).

The pseudo-second-order kinetic model has been based on the premise that sorption occurs due to second-order chemisorption, which may be expressed as the **Eqn. 9**.

$$\frac{t}{q_t} = \frac{t}{k_2 q_e^2} + \frac{t}{q_e} \quad (9)$$

Where k_2 is the second-order rate constant of adsorption (g/mg·min).

H. Thermodynamic Study

Thermodynamics study is very important in adsorption process evaluation to conclude whether the process is spontaneous or not and to ascertain the feasibility study of the process. The thermodynamic parameters include Gibb's free energy change ($\Delta G°$), the change in enthalpy change ($\Delta H°$), and the change in entropy ($\Delta S°$). These are analyzed using **Eqns. 10 & 11** respectively.

$$\Delta G° = -RT \ln K_L \quad (10)$$

$$\ln K_L = \frac{\Delta S°}{R} - \frac{\Delta H°}{RT} \quad (11)$$

The plot of ln K_L against $\frac{1}{T}$ in equation 11 can be used to analyze $\Delta H°$ accordingly, from the intercept and slope.

Where; R represents the universal gas constant (8.314 J/mol.K), T denotes the temperature (K) and K_L represents the Langmuir constant.

III. Results and Discussion

A. Characterization of Nano Adsorbents (FTIR)

The FTIR spectrum of the beneficiated clay (B-clay) is given in Fig. 1a. The Figure shows characteristic short peaks between 3500-3800 cm^{-1} which are indicative of the presence of O-H stretching vibrations of adsorbed water molecules.

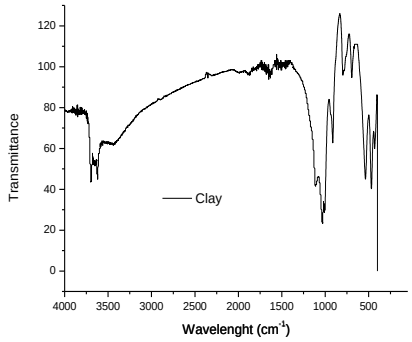

Figure. 1a: FTIR Spectrum of beneficiated clay (B-clay).

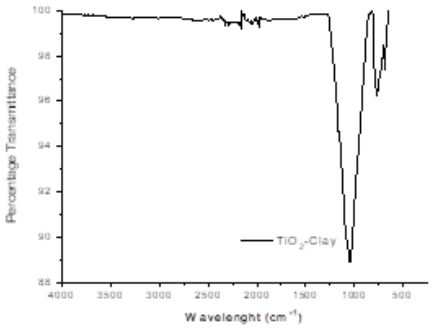

Figure. 1b: FTIR spectrum of TiO_2-clay

The peak at 1624 cm^{-1} also corresponds to the O—H winding vibration of water molecules adsorbed on the surface of kaolinite clay minerals [37]. Si-O-Si and Si-O-Al stretching bands are observed between 1150 and 950 cm^{-1}. Other compounds bonded naturally to the clay are found between 800 and 475 cm^{-1}. According to Fig. 1b, there are several characteristic short peaks between 2500 and 3800 cm^{-1}, which are indicative of –OH bands. The band at 1670 cm^{-1} compared with that at 1624 in Fig Ia, corresponding to the O—H vibration of water molecules adsorbed on the surface of TiO_2-Bclay. The very sharp and intense peak of Si-O-Si and Si-O-Al bands was distinct on 1048 cm^{-1}, representing angular deformations of Si-O-Si and Si-O-Al in the TiO_2-Bclay. Indicative peaks of Ti-O stretching vibrations were observed in the range of 700-875 cm^{-1}which indicates the formation of a metal-oxygen bond. The shift in peaks positions and new peaks observed when Figs. 1a and b are compared, indicating that, TiO_2 nanoparticles have been incorporated with the alumina and silicate particles in the Bclay.

B. XRD

The XRD results in Figs. 2a and b show the crystalline nature of the (a) clay and (b) TiO_2-Bclay. This reveals that the clay and clay composite comprises aluminium, silicon, and titanium dioxide with Bragg's peak at definite 2θ angles. From Fig. 2a, the 2θ diffraction peak at 12.36° (100), 19.92° (020), 35.91° (-131) and 38.40° (-113), which are kaolinites peaks that conform with the JCP 01-079-1570 library.

At 20.91° (100), 26.80° (101) 40.22° (111) and 60.01° (211) are quartz peaks while the scanty short peaks at 24.94°, 28.56° are Albite (Na1.09(Al1.09Si2.91O8)) peaks. Other peaks are at 76.42° and 82.02°, synchronized to calcite-magnesian peaks ($MgO.CaO.CO_3$) as impurities in the clay source.

As shown in Fig. 2b, there are quartz peaks with a reduced intensity which could be due to the TiO_2 doping effects on the clay. The peaks at 27.50°, 36.11°, 41.20°, 54.92°, and 68.38° are titanium (TiO_2) peaks of rutile (JCP2-21-1276) transformations which are well intercalated between the quartz peaks. The peaks 13.02° and 18.62° are Kaolinites transformations to Microcline ($KAlSi_3O$) while other transformations of Kaolinite as Albite ($AlSi_3O_3$) are present at 22.05° and

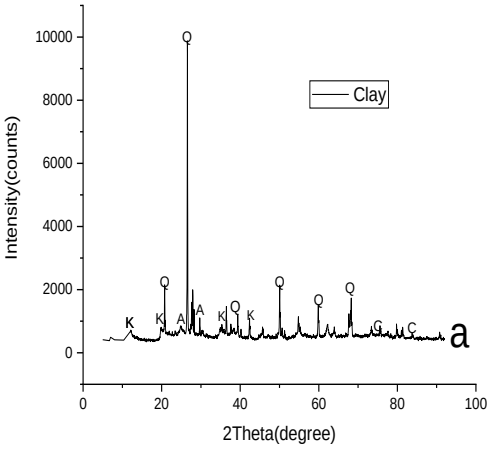

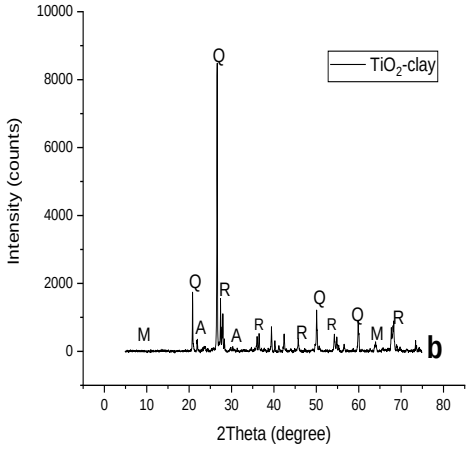

K=Kaolinite, R=Rutile TiO_2, A=Albite, M=Microcline, Q=quartz

Figure. 2(a-b): XRD of (a) Clay (b) TiO_2-clay

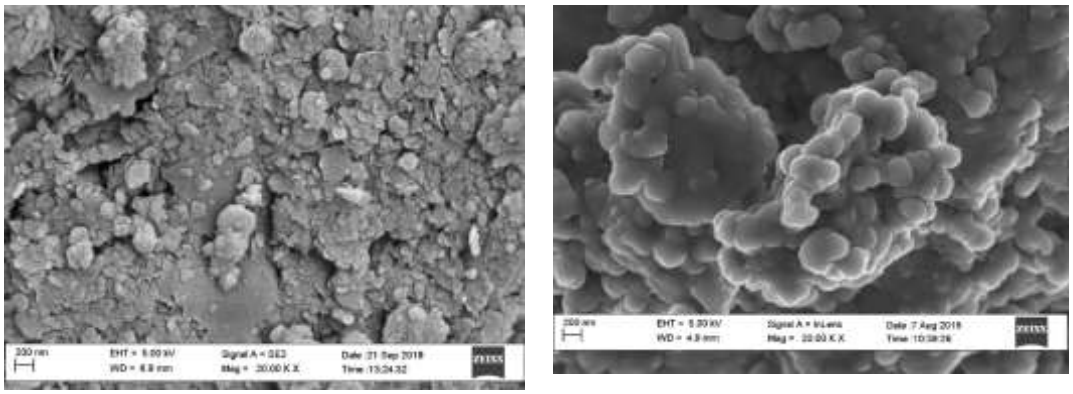

(a) (b)

Figure .3(a-b): SEM of (a) Raw clay (b)TiO_2-Bclay

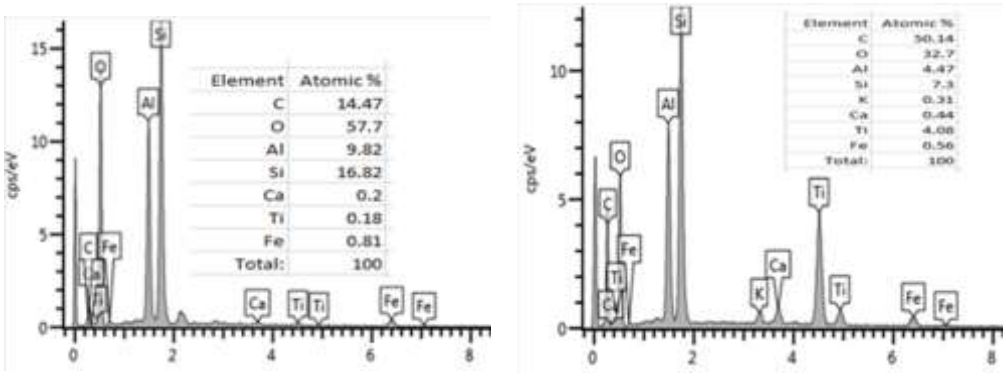

(a) (b)

Fig.4(a-b): EDX of (a) Raw clay (b)TiO2-Bclay

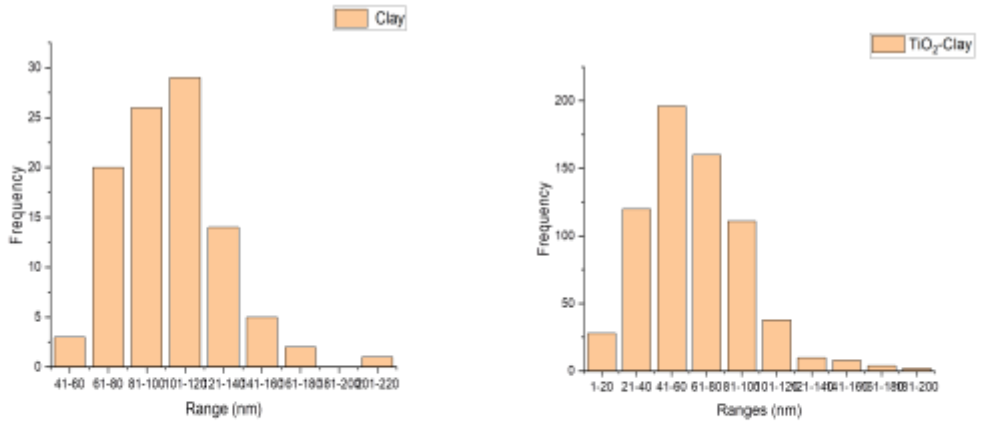

(a) (b)

Figure. 5(a-b): PSD of (a) Raw clay (b)TiO_2-Bclay

28.45°. These transformations are associated with the calcination of the clay composite at 450°C temperature to obtain the TiO_2-Bclay composite. The result confirmed the formation of Alumina, Silicate, and rutile

Titanium dioxide in the synthesized composite.

C. HRSEM, EDS, and PSD Analyses

The HRSEM/EDS analyses of the raw clay and TiO_2-Bclay study consist of the morphology, elemental composition, and particle size distributions (PSD) analyses as shown in Figs. 3-5(a- b). Fig. 3a revealed the morphology of the raw clay showing clusters of irregular hemispherical patterns. These have rough surfaces with attached pores. Fig. 4a presents raw clay EDS, which reveals that the clay particle consists of aluminium, silicon, titanium, iron, calcium, oxygen, and carbon. The EDS elemental composition confirmed that the raw clay is alumino-silicate in nature, which is also a kaolinite mineral present in the line energy of oxygen (0–2 keV), which agrees with previous findings by Mustapha *et al.* [29]. The presence of carbon is traced to adventitious roots and iron to source impurity. Fig. 5a shows the raw clay's particle size distribution (PSD). The PSD shows which particle size range has the most dominance, being 101–120 nm as obtained from the SEM morphology using Image-J particle size distribution calculating software. The finding suggests that the beneficiated clay obtained is a nano-clay of sub-200 nm.

After pillaring the clay with TiO_2 nanoparticles by the wet impregnation method, to obtain TiO_2-Bclay in Fig. 3b, the morphology reveals less agglomeration with an improved smooth surface.

The clusters of spherical morphology reveal small flake-likes with hexagonal structures organized in hemispherical design contrasted well to known kaolinites' crystalline pseudo-hexagonal edges [29]. The hemispherical patterns are in well-repeated patterns and are quite noticeable with random dispersal, porosity, and fewer lumps. The observed patterns are linked to TiO_2 presence on the beneficiated clay's surface and the calcination temperature, leading to the formation of stable titanium (IV) oxide and the porous arrangement of the beneficiated clay lattice. This means the porosity of the prepared nanomaterial will be responsible for the adsorption of intended pollutants.

Fig. 4b presents the TiO_2-clay EDS of the spectrum, showing that the TiO_2-clay conglomerate consists of aluminium, silicon, titanium, iron, calcium, potassium, oxygen, and carbon. The atomic composition of TiO_2 in the clay increased from 0.18 to 4.08% which confirms the impregnation of TiO_2 onto the clay particles, calcium atomic composition increased from 0.20% to 0.44% as a composition of *P. biglobossa* extract utilized in the reduction of TiO_2 nanoparticles. The presence of potassium is also accredited to the aqueous leaves extract used in synthesizing the TiO_2. The PSD of the TiO_2-clay shown in Fig. 5b revealed the domination of particle size range of 41–60 nm which is similar to that obtained from the SEM morphology (Image-J). This finding suggests that the TiO_2-clay is a nanoparticle of sub-100 nm, indicating that, the distribution of particle size present decreases upon heat tempering and doping with the synthesized TiO_2 nanoparticles.

D. Basis for Removal of Zn (II), Pb (II), and Cu (II) in the Aqueous Solution.

Adsorption technology is applicable in industrial wastewater treatment, as such the ultimate goal of this study is to consider an industrial effluent that can be mitigated using a locally developed adsorbent that is made up of TiO_2/clay nanocomposites. Hence, pharmaceutical wastewater was collected from a company in Ilorin, Nigeria which was analyzed for heavy metals, and the results obtained were compared with WHO standards (2008). The concentrations of heavy

metal ions in the pharmaceutical wastewater were analysed by the Atomic Absorption Spectroscopy (AAS) and the results obtained are shown in Table 1. From the table, the concentrations of Zn (II), Pb (II) and Cu (II) are 0.055 mg/L, 0.35 mg/L, and 0.20 mg/L, respectively which are above the permissible limit set by WHO. However, to justify the effectiveness of the developed adsorbent for removal of more concentrated heavy metals ions of Zn (II), Pb (II) and Cu (II) in any pharmaceutical wastewater sources, thus, a higher concentration of Zn (II), Pb (II) and Cu (II) ions were simulated.

E. Effects of Contact Time

The contact time effect on the adsorption of Zn (II), Pb (II), and Cu (II) onto TiO_2-Bclay is presented in **Fig. 6**. Varying the time between 30−240 minutes (30 minutes intervals), at an unchanging concentration of 1000 mg/L, 0.5 g dose of adsorbent, solution pH of 4.5, and 30 ℃ temperature. The percentage adsorption increased steadily from 30 until 90 minutes when there is no supplementary improvement in the percentage of ions sequestered; at this point, equilibrium is ascertained to be reached for the three ions; Zn (II) and Pb (II), and Cu (II). The rapid rate of adsorption before 90 minutes can be accredited to contacts of metal ions with an accessible surface for adsorption. Meanwhile, subsequent steady adsorption is linked with the uptake of metal ions into the pore of the adsorbent [38].

F. Effect of Adsorbent Dosage

The mass of the adsorbent used is important in determining the adsorption competence at a particular initial adsorbate concentration. The increase in adsorbent dosage from 1 to 20 g/L causes a gradual increase in percentage adsorption as shown in **Fig. 7** which can be supported by an increase in active spots on the available adsorbent [39]. Although the increase in percentage adsorption of Zn(II) with the increase in adsorbent dosage was low as compared to adsorption of Pb(II) and Cu(II). Zn(II) ion was readily adsorbed with maximum adsorption of 99.00% at 1 g of adsorbent compared to Pb(II) at 92.51% and Cu(II) at 88.27%. Therefore, it can be deduced that Zn (II) ions have a greater affinity for the Clay-BTiO_2 adsorbent than Pb (II) and Cu (II) ions.

G. Effect of pH

Another important parameter that specifically influences the adsorption process is the solution pH. This is because; it regulates the adsorbents' surface charge and the adsorbate in the solution state. The effect of pH on the uptake of the Pb (II), Cu (II), and Zn (II) metal ions onto TiO_2-Bclay was studied in the range of pH between 2.0 and 10.0**.** From Fig. 8, it is evident that the increase in pH relatively increased the percentage adsorption for Pb (II) and Cu (II). At low pH (< 5), the percentage adsorption is observed low while increased at pH 6 to 95.63% Pb (II), 95.63%

Table 1. Pharmaceutical Wastewater Treatment Result Compared with WHO Standards (2008)

Heavy Metal	Concentration (mg/L)	WHO (2008) standard (mg/L)	Permissible Limit	After adsorption onto TiO_2-Bclay
Fe	0.05	0.30	Below	-
Mn	0.02	0.40	Below	-
Zn	0.055	0.01	Above	0.00
Cd	–	0.003	Below	-
Cu	0.20	2.00	Below	0.00
Pb	0.35	0.01	Above	0.01

Cu (II) 99.54% Zn (II) removal. This is because, at low pH, the surface of TiO_2-Bclay has increased protonation, thereby making the adsorption sites to be charged positively. Also, at the lower pH, there might have been between H^+ and the Zn (II), Pb (II), and Cu (II) for available binding sites, which decreased the expected metal adsorption. On the contrary, at higher pH, deprotonation occurs, which is produced by the presence of too many OH ions in the solution causes the surface of TiO_2-Bclay to become negatively charged [32]. Higher pH may have improved the electrostatic interaction between negatively charged adsorbent surface and heavy metal ions, which are positively charged, boosting the adsorption. As the pH was increased to 10, the percentage of adsorption slightly declined, which could be referred to as a slight desorption process. This infers that an increase in pH above 8 may not be required for effective adsorption of Zn (II), Pb (II), and Cu (II). This evidence is buttressed by the pH point zero charge attainment at pH 8.

H. Effect of Temperature

The impact of temperatures; 30, 40, and 50℃ on the adsorption of Zn (II), Pb (II), and Cu(II) adsorption onto TiO_2-Bclay is presented in Fig. 9. The study revealed that percentage adsorption decreased as the temperature increased for Pb (II) ions, but slightly favourable for Zn (II) ions at 40℃, but worst at 50℃. Optimum adsorption for both ions was attained at 30 ℃ with percentage adsorption up to 88.83% Pb (II) and 99.01% for Zn (II) and 87.41% for Cu (II).

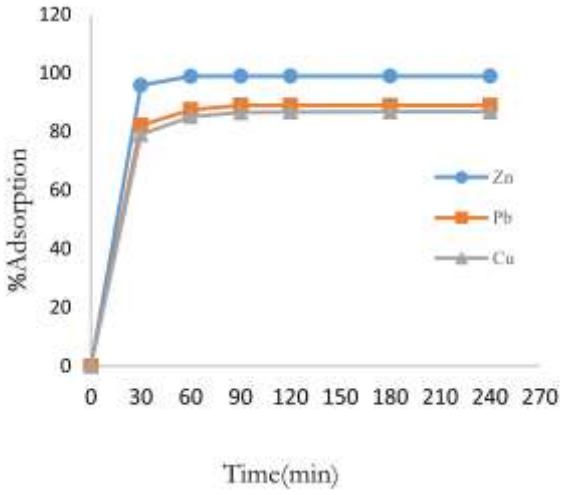

Figure 6: Effect of contact time on Zn (II), Pb (II), and Cu (II) adsorption onto TiO_2 –Bclay.

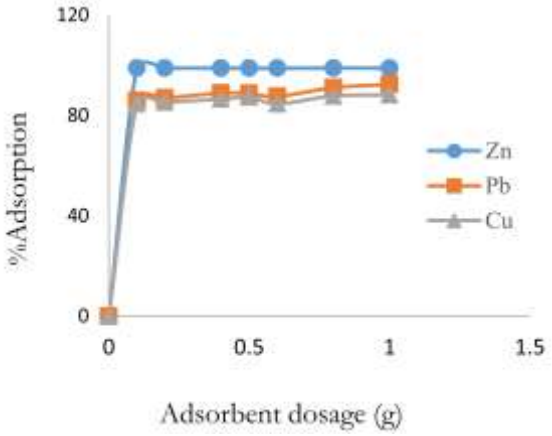

Figure 7: Effect of TiO_2 –Bclay dosage on Zn (II), Pb (II), and Cu (II) adsorption.

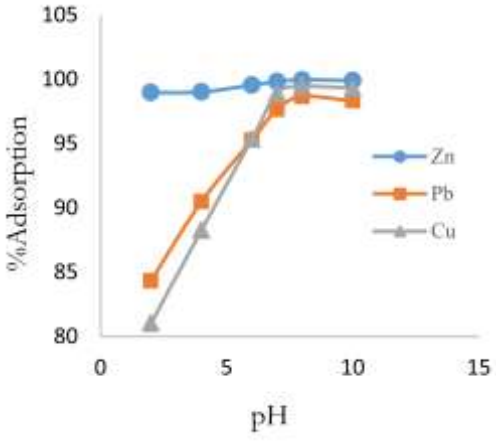

Figure 8: Effect of pH on Zn (II), Pb (II), and Cu (II) adsorption onto TiO_2–clay.

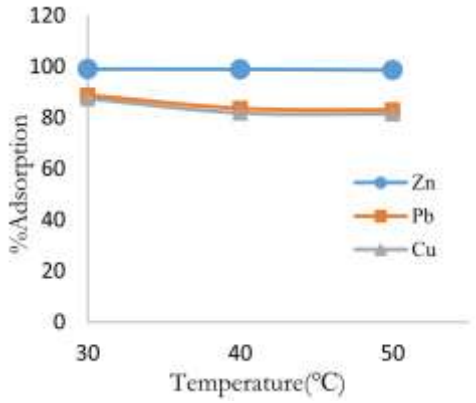

Fig. 9: Effect of temperature on Zn (II), Pb (II), and Cu (II) adsorption onto TiO_2–Bclay

Table 2: Isothermal Parameters of Zn (II), Pb (II), and Cu (II) adsorption onto TiO_2-Bclay

Isotherm models	Zn (II)	Pb (II)	Cu (II)
Langmuir			
K_L	0.0607	0.0171	0.0049
q_m	28.650	33.560	26.390
R^2	0.9873	0.9839	0.9481
Freundlich			
K_f	6.0406	3.7985	1.2188
n	3.8926	2.9472	2.3111
$\frac{1}{n}$	0.2569	0.3393	0.4327
R^2	0.8536	0.8590	0.9692
Dubinin-Radushkevich			
q_{mDR}	25.810	26.780	16.690
K_{DR}	2×10^{-5}	7×10^{-5}	3×10^{-4}
E	5.0000	2.6700	1.2900
R^2	0.8584	0.8803	0.7974
Temkin			
b_T	548.63	413.68	477.08
K_T	1.1034	-1.2473	-2.7631
R^2	0.8554	0.8945	0.9393

I. Adsorption Isotherm Modelling

Freundlich, Langmuir, Dubinin-Radushkevitch, and Temkin's isothermal models were applied to study the adsorption mechanism on the TiO_2-Bclay. Comparison of regression (R^2) values as presented in Table 2 leads to selecting an acceptable adsorption isotherm model for the adsorption of the examined ions by TiO_2-Bclay. The R^2 values of nearly 1 for the ions are evidence that the model can appropriately fit the experimental data. This assessment reveals that the adsorption process isotherms of Zn (II), and Pb (II) can be better described by the Langmuir isothermal model, while for the adsorption of Cu (II), where a R^2 value of 0.9481 for Langmuir isotherm and a R^2 value of 0.9692 for Freundlich isotherm is obtained. The adsorption can be more described by the Freundlich model which establishes that there is no limit to the adsorption ability of the adsorbent. R_L values at temperatures 30°C, 40°C, and 50°C are almost equal to 1, which indicates the adsorption is favourable. Also, from Table 4, the q_m values of the Langmuir isotherm at 30°C which are the maximum amount of metal ion per unit mass of adsorbent required to form a monolayer on the surface shows maximum adsorption in the direction of magnitude Pb (II) > Zn (II) > Cu (II).

J. Kinetics Study

Adsorption kinetics and equilibrium are the two main metrics used to assess adsorption dynamics. The experimental results were utilized to calculate the kinetic constants of Zn (II), Pb (II), and Cu (II) ions adsorption, which could be used to optimize the residence time of industrial wastewater treated with TiO_2-Bclay. At a contact time of 90 min, the adsorption equilibrium was reached. With pseudo-first-order adsorption model, R^2 values of 0.999, 0.978, and 0.991 were obtained for Zn (II), Pb (II), and Cu (II) ions respectively as shown in Fig. 10, while the rate constants are 0.121 min^{-1}, 0.068 min^{-1} and 0.070 min^{-1}. The Pseudo-second-order gave the coefficient of regression (R^2) values of 1.000, 0.999, and 0.999 for the three ions, which are close to unity with the rate constants of 0.032 $gmg^{-1}min^{-1}$, 0.011 $gmg^{-1}min^{-1,}$ and 0.009 $gmg^{-1}min^{-1}$ for the Zn (II), Pb (II) and Cu (II) ions respectively as shown on Fig. 11. This shows a better fit with 90 minutes pseudo-second-order when compared with the pseudo-first-order regression values which are lower.

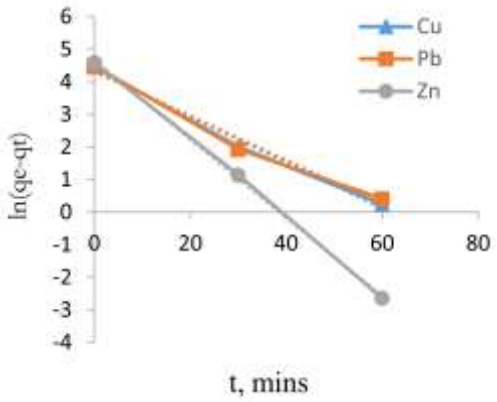

Fig.10: Pseudo-first order model for Zn(II),

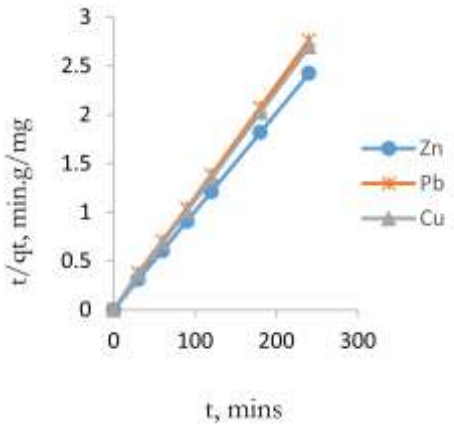

Fig.11: Pseudo-second order model for Zn(II), Pb(II), and Cu(II) adsorption.

Also, the values of q_e obtained from the plot of the pseudo-second-order model is closer to the experimental values than the q_e values obtained in the pseudo-first-order model. Moreover, the error functions; the sum of square error (SSE), the non-linear Chi-square test (χ^2), Average Relative Error (ARE), Root Mean Square Error (RMSE), statistical error analysis values are closer to zero for the pseudo-second-order fit. In contrast, the values obtained from pseudo-first-order are larger, as presented in Table 3. It has been stated that the closer the error function values are to zero, the better the model [40]. These further confirm the suitability of pseudo-second-order as suitable for describing the kinetics of the adsorption of Zn (II), Pb (II), and Cu (II) ions onto the TiO_2-Bclay composite. These results imply that the magnitude of adsorption is the order Zn > Pb > Cu. Whereas the rate-limiting stage is surface adsorption, which involves chemisorption, in which physicochemical interactions cause the removal of the heavyweight metal ions from a solution.

K. Thermodynamic Study

The thermodynamic adsorption parameters are shown in **Table 4**. Change in Gibbs free energy, $\Delta G°$ values obtained were negative, indicating that this adsorption process is thermodynamically feasible and spontaneous. The $\Delta G°$ values for Zn (II) ascended with temperature. Therefore, the adsorption of Zn (II) onto TiO_2-Bclay is favoured by lower

Table 3: Kinetics Model Parameters for the Adsorption Process

Pseudo first order								
Heavy Metal	**q_e(mg/g) experiment**	**q_e(mg/g)**	**k_1(min^{-1})**	**R^2**	**SSE**	**X^2**	**ARE**	**RMSE**
Zn	99.00	104.48	0.121	0.999	30.03	0.30	3.37	1.37
Pb	89.00	74.71	0.068	0.978	204.20	2.29	25.49	3.57
Cu	86.45	77.14	0.070	0.991	86.67	1.00	11.14	2.33
Pseudo second order								
Heavy Metal	**q_e(mg/g) experiment**	**q_e(mg/g)**	**k_2(gmg^{-1}.min)**	**R^2**	**SSE**	**X^2**	**ARE**	**RMSE**
Zn	99.00	99.01	0.0319	1.000	1.0×10^{-4}	1.0×10^{-6}	1.12×10^{-5}	0.0025
Pb	89.00	89.29	0.0107	0.9999	0.08	9.4×10^{-4}	1.0×10^{-2}	0.07
Cu	86.45	87.72	0.0087	0.9999	1.61	0.018	0.21	0.32

temperatures while adsorption of Pb (II) and Cu (II) onto TiO_2-clay is favoured by higher temperatures.

Table 4. Thermodynamic Parameters Evaluated for the Adsorption Process

Heavy metals	ΔH°	ΔS°	ΔG°		
T(°C)			30°C	40°C	50°C
Zn	11.53	10.56	−7.06	−6.64	−6.21
Pb	−71.22	−11.45	−10.25	−10.93	−12.37
Cu	−78.23	−10.44	−13.40	−14.06	−15.60

The negative values of ΔH° for Pb (II) and Cu (II) indicated that the adsorption process was exothermic while for Zn (II), ΔH° was positive, which showed endothermic adsorption, similar to the findings of Chaudry *et al.* [41], who adsorbed Pb (II) and Zn (II) ions into manganese oxide-coated sand. The negative values of ΔS° for Pb (II) and Cu (II) indicated that the adsorption process was not disorderly while for Zn (II), ΔS° was positive which, suggests increasing disorder during the adsorption process, at the solid/liquid interfacial point.

The thermodynamic adsorption parameters of Zn(II) are associated with positive ΔS° values and negative ΔG° values which indicates that there is a high affinity between the adsorbent and adsorbate [42].

L. Evaluation of the Nano-adsorbent.

Table 5 compares the maximum adsorption capacities of several materials and nano-adsorbents used to sequester various pollutants, especially metal ions from different wastewater solutions. It can be observed that most kinetics studied involving TiO_2 composites mostly agrees with Pseudo-second-order kinetics, while their isothermal studies were Langmuir fitted. The high percentage removal of the metal ion by the synthesized nano-adsorbent showed that the TiO_2-Bclay nano-composites were more suitable and effective as a nano-adsorbent for the sequestering of Zn (II), Pb (II), and Cu (II) from the pharmaceutical wastewater than previously reported nano-adsorbents. Also, the contact time in this report was much lower than the most reported, with high percentage removal of 99%, 92%, 88% for Zn (II), Pb (II), and Cu (II) respectively, availability of the natural kaolinite clay, the non-toxic character of the developed nanocomposites accords the TiO_2-BClay a promising and worthwhile adsorbent. The obtained results from the study show the efficacy of TiO_2-BClay nano-composites for heavy metals in pharmaceutical industry wastewater and its suitability for other industrial effluents treatments.

IV. Conclusion

The synthesis of titanium nanoparticles from the plant extract of *Parkia biglobosa* leaves extract using titanium tetrahydroxide as a precursor was achieved. The TiO_2 nanoparticles were supported on beneficiated clay and were used in the adsorption of Zn (II), Pb (II), and Cu (II) ions from simulated aqueous solution. The study concludes that the developed adsorbent was efficient for the removal of Zn (II), Pb (II), and Cu (II) ions in an aqueous solution. As such pharmaceutical wastewater laden with low or high concentrations of the heavy metals (Zn (II), Pb (II), and Cu (II) ions) can be treated with the adsorbent. The conditions of the adsorption process studied; contact time, pH, adsorbent dosage, and temperature were found to have a significant effect on the adsorption process with the highest percentage adsorption obtained at pH 8 compared to low pH of 2. Adsorption of the Zn (II), Pb (II), and Cu (II) adsorption was

Table 5: Comparison of Different Adsorbents of TiO_2 Composition, Adsorption Parameters, and their Maximum Percentage Removal of Heavy Metals

Adsorbent	Heavy metal	Adsorption parameters	%Removal	Isotherms and Kinetics	References
TiO_2-Bclay	Zn(II), Pb(II), Cu(II)	m = 0.5g; ads =100 to 1000 mg/L ; T = 30℃	99% 92% 88%	Langmuir; pseudo-second-order	This study
Fe_3O_4@TiO_2-CN	Ni(II), Pb(II)	m = 3g/L; ads = 5 to 500 mg/L T = 45℃	70% 90%	Langmuir; Pseudo-second order	[43]
SSC/ TiO_2/ ZnO nanofiber	Ni(II), Cu(II)	m = 0.5g/L; ads =5 to 500 mg/L; T = 25℃	78% 92%	Langmuir; Pseudo-second order	[44]
TiO_2/Kaolinite Nanocomposite	Pb(II), Cd(II)	m = 0.5g; ads =5 to 80 mg/L	94% 88%	Langmuir	[31]
CBK/TiO_2	Fe	100 mg, 20 mL, 60 min and 22°C	87%	Langmuir, Pseudo-second order	[45]
LDHs/TiO_2	Methyl orange	100 mg, 25°C	90%	Langmuir, Pseudo-first order	[46]
TiO_2//$AgNO_3$ Modified diatomaceous ceramic adsorbent	Cu(II), Co(II)	ads =100 to 1000 mg/L	-	Langmuir; Pseudo-second order	[6]
TiO_2@GAC	Cu(II)	m = 0.5g; ads = 5 to 80 mg/L	78.9%	Langmuir; Pseudo-second order	[47]
Talc/TiO_2	Th	M= 0.5g, 1000mg/g, 55℃	94.5%	Langmuir; Pseudo-second order	[48]
CeO_2–$TiFe_2O_4$	U (IV)	0.005g, 20 mg L^{-1}, 120 min, 25 °C	89.8%	Langmuir; Pseudo-second order	[49]
TiO_2	Pb (II)	0.15 g, 240 min, 25	82.5%	Langmuir; PSD	[15]

Key: M= adsorbent dosage, T=temperature, t= time C=Initial concentration, Lang=Langmuir,

obtained at 90 min equilibrium time. The prepared adsorbate solution containing 1000 mg/L was treated using 20 g/L of adsorbent, percentage removal up to 99.00% Zn(II), 92.51% Pb(II), and 88.27% Cu(II) ions at 30 ℃ were achieved. The adsorption process fits into the Langmuir isotherm for Zn(II) and Pb(II) and Freundlich isotherm for Cu(II). The adsorption kinetics fit into the pseudo-second-order model, implying that the rate-limiting phase is surface adsorption, which involves chemisorption and requires physicochemical interactions to remove from the solution. The enthalpy changes 11.53, −71.22, and -78.23 kJ/mol for Zn (II), Pb (II), and Cu (II) ions affirms the endothermic and exothermic forms of the adsorption. The results showed that TiO_2-clay is suitable for adsorption of heavy metals like Zn (II), Pb (II) and Cu (II) in wastewater as the solution, with a greater affinity for Zn (II) and Pb (II) ions. Therefore, the locally sourced,

beneficiated alumino-silicate clay modified with TiO_2 is an effective adsorbent for heavyweight metals and advantageous for other industrial wastewater applications.

References

[1] Bai, S.H. and Ogbourne, S.M. "Glyphosate: Environmental Contamination, Toxicity and Potential risks to Human Health via Food Contamination", *Environmental Science Pollution Resources*, vol. 23, 2016, pp. 18988–19001.

[2] Azizi, S.M., Shahri, M. and Mohamad, R. "Green Synthesis of Zinc Oxide Nanoparticles for Enhanced Adsorption of Lead Ions from Aqueous Solutions: Equilibrium, Kinetic and Thermodynamic Studies", *Molecules*, vol. 22, no. 6, 2017, pp. 831-850.

[3] Balali-Mood, M., Naseri, K., Tahergorabi, Z., Khazdair, M.R. and Sadeghi, M. "Toxic Mechanisms of Five Heavy Metals: Mercury, Lead, Chromium, Cadmium, and Arsenic", *Frontiers in Pharmacology,* vol. 12, no. 643972, 2021, pp. 1-19, doi:10.3389/fphar.2021.643972

[4] Akpor, O.B., Ohiobor, G.O. and Olaolu, D. "Heavy Metal Pollutants in Wastewater Effluents: Sources, Effects and Remediation", *Advances in Bioscience and Bioengineering*, vol. 2, no. 4, 2014, pp. 37-43.

[5] Gebru, K.A. and Das, C. "Removal of Pb (II) and Cu (II) ions from Wastewater using Composite Electrospun Cellulose Acetate/titanium Oxide (TiO_2) Adsorbent", *Journal of Water Process Engineering*, vol. 16, 2017, pp. 1-13.

[6] Ajenifuja, E., Ajao, J. and Ajayi, E. "Adsorption Isotherm Studies of Cu (II) and Co (II) in High Concentration Aqueous Solutions on Photo-catalytically Modified Diatomaceous Ceramic Adsorbents", *Applied Water Science*, vol. 7, no. 7, 2017, pp. 3793-3801.

[7] Mustapha, S., Ndamitso, M.M., Abdulkareem, A.S., Tijani, J.O., Shuaib, D.T., Ajala, A.O. and Mohammed, A.K. "Application of TiO_2 and ZnO Nanoparticles Immobilized on Clay in Wastewater Treatment: A Review", *Applied Water Science,* vol. 10, no. 49, 2020, pp. 1-36, doi:10.1007/s13201-019-1138-y

[8] Nilchi, A., Dehaghan, T.S. and Garmarodi S.R. "Kinetics, Isotherm and Thermodynamics for Uranium and Thorium Ions Adsorption from Aqueous Solutions by Crystalline Tin Oxide Nanoparticles", *Desalination*, vol. 321, 2013, pp. 67-71.

[9] Lai, K.C. "Facile Synthesis of Xanthan Biopolymer Integrated 3D Hierarchical Graphene Oxide/titanium Dioxide Composite for Adsorptive Lead Removal in Wastewater", *Bioresource Technology*, vol. 309, no. 123296, 2020. pp. 1-18.

[10] Yang, S., Xiao, X. and Tao, E. "Removing Low Concentration of Cr (III) from Wastewater: Using Titanium Dioxide Surface-modified Montmorillonite as a Selective Adsorbent", *Inorganic Chemistry Communications*, vol. 125. no. 108464, 2021.

[11] Ksakas, A. "Removal of Cu (II) Ions from Aqueous Solution by Adsorption using Natural Clays: Kinetic and Thermodynamic Studies", *Journal of Materials and Environmental Science,* vol. 9 no. 3, pp. 1075-1085.

[12] Shama, S. and Gad, M. "Removal of Heavy Metals (Fe^{3+}, Cu^{2+}, Zn^{2+}, Pb^{2+}, Cr^{3+} and Cd^{2+}) from Aqueous Solutions by using Hebba Clay and Activated Carbon", *Portugaliae Electrochimica Acta*, vol. 28 no. 4, 2010. pp. 231-239.

[13] Ogunleye, O.O., Ajala, M.A. and Agarry, S.E. "Evaluation of Biosorptive Capacity of Banana (Musa paradisiaca) Stalk for Lead(II) Removal from Aqueous Solution", *Journal of Environmental Protection*, vol. 5, 2014. pp. 1451-1465.

[14] Sharma, S. et al., "Physical, Chemical and Phytoremediation Technique for Removal of Heavy Metals", *Journal of Heavy Metal Toxicity and Diseases,* vol.1, no. 2, 2016. pp. 1-15.

[15] Poursani, A.S. et al., "The Synthesis of Nano TiO_2 and its use for Removal of Lead Ions from Aqueous Solution", *Journal of Water Resource and Protection*, vol. 8, no.04 2016, pp. 438-442.

[16] Liang, R. et al., "Fundamentals on Adsorption, Membrane Filtration, and Advanced Oxidation Processes for Water Treatment, in Nanotechnology for Water Treatment and Purification, 2014, *Springer,* pp. 1-45.

[17] Ajala, E.O., Ajala, M.A. and Saka H.B. "Titanium Dioxide-based Nanocatalyst in Biodiesel Production, in Nano- and Biocatalysts for Biodiesel Production", *A.P. Ingle, Editor. John Wiley & Sons Ltd.: Hoboken, New Jersey, USA,* 2021, pp. 115-142.

[18] Annan, E. et al., "Application of Clay Ceramics and Nanotechnology in Water Treatment: A Review", *Cogent Engineering,* 2018. Vol. 5, no. 1, pp. 1476017.

[19] Guillaume, P.L.A., Chelaru, A., Visa, M. and Lassiné, O. "Titanium Oxide-clay as Adsorbent and Photocatalysts for Wastewater Treatment", *Journal of Membrane Science and Technology*, vol. 8, no. 1, 2018. pp. 176-186.

[20] Sharififard, H., Ghorbanpour, M. and Hosseinirad, S. "Cadmium Removal from Wastewater using Nano-clay/TiO_2 Composite: Kinetics, Equilibrium and Thermodynamic Study", *Advances in Environmental Technology*, vol. 4, no. 4, 2018, pp. 203-209.

[21] Noruzi, M. "Biosynthesis of Gold Nanoparticles using Plant Extracts", *Bioprocess and biosystems engineering,* vol. 38, no. 1, 2015, pp. 1-14.

[22] Pushpamalini, T. "Comparative Analysis of the Green Synthesis of TiO_2 Nanoparticles using Four Different Leaf Extract", *Materials Today: Proceedings,* vol. 40, 2021. pp. S180-S184.

[23] Swathi, N. "Green Synthesis of Titanium Dioxide Nanoparticles using Cassia Fistula and its Antibacterial Activity", *International Journal of Research In Pharmaceutical Sciences,* vol. 10, no. 2, 2019. pp. 856-860.

[24] Thakur, B.K., Kumar, A. and Kumar, D. "Green Synthesis of Titanium Dioxide Nanoparticles using Azadirachta Indica Leaf Extract and Evaluation of their Antibacterial Activity", *South African Journal of Botany*, vol. 124, 2019, pp. 223–227.

[25] Dobrucka, R. "Synthesis of Titanium Dioxide Nanoparticles using Echinacea Purpurea Herba", *Iranian Journal of Pharmaceutical Research,* vol 16, no. 2, 2017, pp. 756-762.

[26] Madadi, Z., Soltanieh, M., Lotfabad, T.B. and Nazari, B.S. "Green Synthesis of Titanium Dioxide Nanoparticles with Glycyrrhiza Glabra and their Photocatalytic Activity", *Asian Journal of Green Chemistry*, vol. 4, no. 3, 2020, pp. 256-268.

[27] Ajala, M.A., Abdulkareem, A.S., Tijani, J.O. and Kovo, A.S. "Adsorptive Behaviour of Rutile Phased Titania Nanoparticles Supported on Acid-modified Kaolinite Clay for the Removal of Selected Heavy Metal Ions from Mining Wastewater", *Applied Water Science*, vol. 12, no. 19, 2022, pp. 1-24.

[28] Mishra, A., Mehta, A. and Basu, S. "Clay Supported TiO_2 Nanoparticles for Photocatalytic Degradation of Environmental Pollutants: A Review", *Journal of Environmental Chemical Engineering,* vol. 6, no. 6, 2018, pp. 6088-6107.

[29] Mustapha, S., Ndamitso, M.M., Abdulkareem, A.S., Tijani, J.O., Mohammed, A. K. and Shuaib, D.T. "Potential of using Kaolin as a Natural Adsorbent for the Removal of Pollutants from Tannery Wastewater", *Heliyon*, vol. 5, no. e02923, 2019. pp. 1-17.

[30] Mahy, J.G. "Natural Clay Modified with ZnO/TiO_2 to Enhance Pollutant Removal from Water", *Catalysts*, vol. 12, no. 148, 2022. pp. 1-14.

[31] Awwad, A., Amer, M. and Al-aqarbeh, M. "TiO_2-kaolinite Nanocomposite Prepared from the Jordanian Kaolin clay: Adsorption and Thermodynamics of Pb (II) and Cd (II) ions in Aqueous Solution", *Chemistry International*, 2020.

[32] Hajjaji, W. "Effective Removal of Anionic and Cationic Dyes by Kaolinite and TiO2/kaolinite Composites", *Clay Minerals*, vol. 51, no. 1, 2018. pp. 19-27.

[33] Zahir, A.A. "Green Synthesis of Silver and Titanium Dioxide Nanoparticles using Euphorbia Prostrata", *Antimicrobial Agents and Chemotherapy,* vol. 59, no. 8, 2015. pp. 4782-4799.

[34] Laysandra, L. "Adsorption and Photocatalytic Performance of Bentonite-titanium Dioxide Composites for Methylene Blue and Rhodamine B Decolouration", *Heliyon,* vol. 3, 2017, pp. 1-22.

[35] Freundlich, H. "Over the Adsorption in Solution", *Journal of. Physical Chemistry*, vol. 57**,** no**.** 385471, 1906, pp. 1100-1107.

[36] Langmuir, I. "The Adsorption of Gases on Plane Surfaces of Glass, Mica and Platinum", *Journal of the American Chemical Society*, vol. 40, no. 9, 1918 pp. 1361-1403.

[37] Diko, M., Ekosse, G. and Ogola, J. "Fourier Transform Infrared Spectroscopy and Thermal Analyses of Kaolinitic Clays from South Africa and Cameroon", *Acta Geodyn. Geomater*, vol. 13, no. 182, 2016, pp. 149–158.

[38] Adebayo, G., Adegoke, H. and Fauzeeyat, S. "Adsorption of Cr (VI) Ions onto Goethite, Activated Carbon and their Composite: Kinetic and Thermodynamic Studies", *Applied Water Science*, vol. 10, no. 9, 2020, pp. 1-18.

[39] Inyinbor, A.A., Adekola, F.A. and Olatunji, G.A. "Kinetics, Isotherms and Thermodynamic Modelling of Liquid-phase Adsorption of Rhodamine B dye onto Raphia Hookeriem Fruit Epicarp", *Water Resources and Industry,* vol. 15, 2016, pp. 14-27.

[40] Egbosiuba, T.C. "Enhanced Adsorption of As(V) and Mn(VII) from Industrial Wastewater using Multi-walled Carbon Nanotubes and Carboxylated Multi-walled Carbon Nanotubes*", Chemosphere,* vol. 254, no. 126780, 2020.

[41] Chaudhry, S.A., Khan, T.A. and Ali, I. "Adsorptive Removal of Pb(II) and Zn(II) from Water onto Manganese Oxide-coated Sand: Isotherm, Thermodynamic and Kinetic Studies"*, Egyptian Journal of Basic and Applied Sciences,* vol. 3, 2016, pp. 287–300.

[42] Miyah, Y. "Assessment of Adsorption Kinetics for Removal Potential of Crystal Violet Dye from Aqueous Solutions using Moroccan Pyrophyllite"*, Journal of the Association of Arab Universities for Basic and Applied Sciences*, vol. 23, 2017, pp. 20-28.

[43] Mousavi, S.V. "A Novel Cyanopropylsilane-functionalized Titanium Oxide Magnetic Nanoparticle for the Adsorption of Nickel and Lead Ions from Industrial Wastewater: Equilibrium, Kinetic and Thermodynamic Studies"*, Microchemical Journal*, vol. 145, 2019, pp. 914-920.

[44] Khosravi, M. "Synthesis of TiO_2/ZnO Electrospun Nanofibers Coated-sewage Sludge Carbon for Adsorption of Ni(II), Cu(II), and COD from Aqueous Solutions and Industrial Wastewaters*", Journal of Dispersion Science and Technology*, vol. 42, no. 6, 2021, pp. 802-812.

[45] Hana, Y. "Functionalizing Naturally Occurring Kaolinite by Anatase Nanoparticles and its Effects on the Adsorption of Fluoride", *Desalination and Water Treatment*, vol. 160, 2019, pp. 240-249.

[46] Suh, M. "Titanium Dioxide−layered Double Hydroxide Composite Material for Adsorption−photocatalysis of Water Pollutants"*, Langmuir*, vol. 2019, no. 35, 2019, pp. 8699−8708.

[47] Zheng, X. "Adsorption Properties of Granular Activated Carbon-supported Titanium Dioxide Particles for Dyes and Copper Ions", *Scientific reports*, vol. 8, no. 1, 2018, pp. 1-9.

[48] Morsy, A. "Performance of Magnetic Talc Titanium Oxide Composite for Thorium Ions Adsorption from an Acidic Solution"*, Environmental Technology & Innovation*, vol. 8, 2017, pp. 399-410.

[49] El-Said, A.N. "CeO_2–$TiFe_2O_4$ Nanocomposite for Effective Removal of Uranium Ions from Aqueous Waste Solutions"*, SN Applied Sciences*, vol. 1, no.2, 2019. pp. 159.